THE JOURNAL OF PHYSICAL CHEMISTRY B

Article

pubs.acs.org/JPCB

Hydrogen Bonds and Heat Diffusion in α-Helices: A Computational Study

German Miño,*[,†,‡,§] Raul Barriga,[†] and Gonzalo Gutierrez[†]

[†]Group of NanoMaterials, Departamento de Física, Facultad de Ciencias, Universidad de Chile, Casilla 653, Santiago, Chile

[‡]Centro Interdisciplinario de Neurociencias de Valparaíso (CINV), Universidad de Valparaíso, Valparaíso, Chile

[§]Facultad de Ciencias Biologicas, Centro de Bioinformatica y Biologia Integrativa, Universidad Andres Bello, Av.Republica 239, Santiago, Chile

ABSTRACT: Recent evidence has shown a correlation between the heat diffusion pathways and the known allosteric communication pathways in proteins. Allosteric communication in proteins is a central, yet unsolved, problem in biochemistry, and the study and characterization of the structural determinants that mediate energy transfer among different parts of proteins is of major importance. In this work, we characterized the role of hydrogen bonds in diffusivity of thermal energy for two sets of α-helices with different abilities to form hydrogen bonds. These hydrogen bonds can be a constitutive part of the α-helices or can arise from the lateral chains. In our in vacuo simulations, it was observed that α-helices with a higher possibility of forming hydrogen bonds also had higher rates of thermalization. Our simulations also revealed that heat readily flowed through atoms involved in hydrogen bonds. As a general conclusion, according to our simulations, hydrogen bonds fulfilled an important role in heat diffusion in structural patters of proteins.

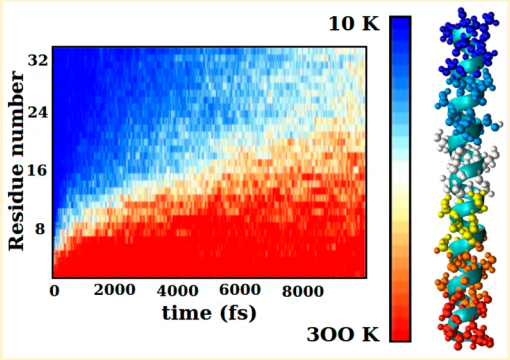

INTRODUCTION

Proteins play the most important role in living organisms. In this respect, energy transport in proteins is an open problem in biochemistry that involves important topics conformational changes, enzyme catalysis, allosteric cooperativity, and intermolecular affinities, among other process.[1] The necessary biological energy can originate from several sources such as thermal gradients, chemical or photochemical changes in substrates at active sites of enzymes, or protein−ligand binding.[1] In that respect, nonlinear excitations such as breathers,[2] solitons,[3−5] low- and high-energy vibrational modes[1,6] have been drawing increasing attention as mediators of energy transport in biomolecules.

Due their polymeric nature, when proteins fold to reach their biological active state, they generate a complex network of contacts. Previous reports have shown that thermal energy flows in proteins according to the physical connectivity of this network,[7,8] with velocities of propagation in the orders of 10 Å ps^{-1}.[6] This flow of thermal energy mimics the heat transport of percolation clusters, where the energy flows anisotropically, that is, fast along physically connected channels and rather slow along numerous pathways that reach dead-ends.[6] Recent evidence has shown a correlation between the heat diffusion pathways and the known allosteric communication pathways in proteins.[9−11] Allosteric communication determines the processes of signal transmission through proteins, on both short (3 Å) and long (100 Å) range scales. This phenomenon is involved in crucial cellular and physiological functions and is a determinant for serious human diseases.[12−14,41] Allosteric communication can be determined using both experimental[15−21,26,27] and theoretical[1,6−11,19,22−25] techniques, and their occurrence has been clearly established.

Large efforts have been made to study the energy flow in proteins and its relation in protein dynamics.[28−33,36] Research on heat flow in different structures, such as peptide helices,[31] heme cofactors,[32] beta sheets[33] and functionalized materials[34,35] have been reported in literature. These reports have shown that the excess of energy deposited in particular sites can propagate along the structures through the covalent backbone of the molecules[31,35] and also through weaker interactions, such as hydrogen bonds.[33,34] Additionally, the energy deposited in particular sites can flow toward the solvent.[31] The solvent can play an important role in energy diffusion through the proteins, as in the Ca^{2+} ATPase;[28,29] at the surface of proteins, as in PDZ-2 domain[27] and between protein subunits, as in hemoglobin.[8]

Hydrogen bonds have been an inexhaustible source of research for decades.[37] Their role as stabilizing agents of protein structure have been clearly established.[38] Also, they act in the modulation chemical reactivity in proteins[43−45] and, as has been earlier proposed from the field of physics, can act as energy carriers in protein structures.[3] In this regard, the role of hydrogen bonds in thermal conduction, has been recently reported, revealing their importance in heat diffusion across of β-sheet structure of the spider silk protein.[33] In a similar way Martinez et al.[40] have shown

Received: April 7, 2014
Revised: July 13, 2014
Published: August 8, 2014

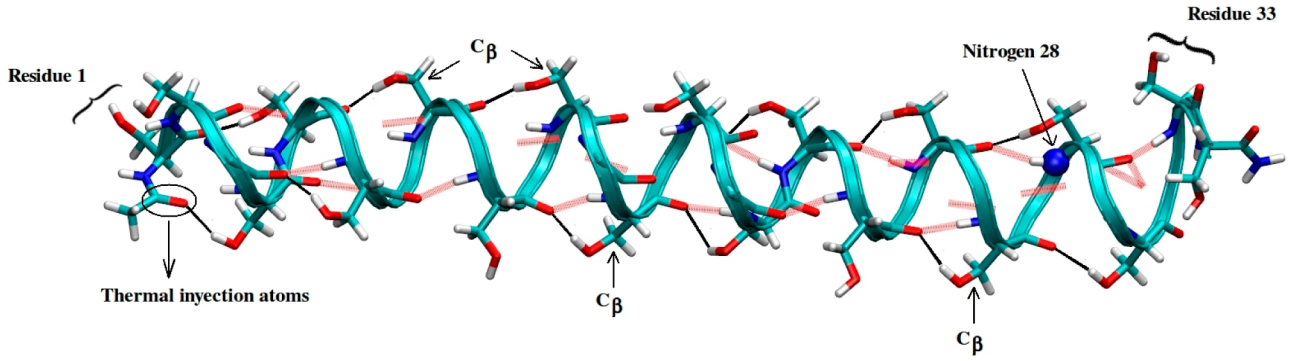

Figure 1. Model for polyserine. The thick red dashed lines represent the central hydrogen bonds that stabilize the helical structure. The thin black dashed line represents lateral hydrogen bonds that are formed by the lateral chains. For some lateral chains, C_β is indicated, and nitrogen 28 is depicted as a reference.

that residues, such as arginine, lysine, aspartate, and glutamate, are responsible for the vibrational energy flow among segments of the binding domains in thyroid hormone receptors. Moreover, the mutation of these key residues severely impaired the functionality of these receptors. Due to their charged nature, these residues can form charge-assisted hydrogen bonds,[41] in addition to also having the potential to form short hydrogen bonds.[42] The role that short hydrogen bonds have in the enhanced catalytic properties of proteins has been experimentally studied,[43] while theoretical studies have examined their electronic properties and the effect that they have on the chemical reactivity of surrounding structural elements.[44,45] Keeping in mind the significance of allosteric communication in proteins, the study and characterization of structural determinants that mediate energy transfer among different parts of proteins is of major importance.

Interestingly, there exists a model regarding the role of hydrogen bonds in heat diffusion in peptide helices, the so-called Davydov model.[3] This model describes how the released energy from, e.g., ATP hydrolysis, is trapped and how it then propagates along peptide helices. The released energy is captured by the amide I vibrational mode of the nearby peptide groups (CONH) of the helix. Peptide groups give rise to the hydrogen bonds that stabilize the peptide helix. The amide I vibrational mode included a major component from the stretching of carbonyl group (CO), and relatively small components from both the C−N in-plane stretching and N−H in-plane bending vibration. The excitation of amide I modes provokes a local deformation of the helix. The interplay between the deformation and excitation creates a wave that propagates along the structure, a soliton.[3−5] Some authors have made research based on this hypothesis, e.g., refs 3 and 4, nevertheless its validity at relevant biological temperatures has been put in doubt.[39]

In this work, we characterized the role of hydrogen bonds in the heat diffusion of α-helices. Using a molecular dynamics simulation for a set of α-helices, we estimated the energy flux at selected points of the structure. The results were analyzed in terms of the chemical nature of the α-helix building blocks; that is, in terms of their ability to form hydrogen bonds and on the length of the lateral chain. Increased thermal diffusivity was found in structures that presented a shorter lateral chain and that formed extra hydrogen bonds. Our results are in direct concordance with recent reports about the role of hydrogen bonds in the enhanced heat diffusion in structural patterns of proteins, such as β-sheets[33] and in other functionalized materials.[34]

METHODS AND COMPUTATIONAL DETAILS

The evaluation of thermal conductivity was performed for 10 α-helical structures, five of which presented nonpolar lateral chains and five of which presented polar lateral chains. Each α-helix was composed by only one type of amino acid residue, and each had a length of 33 residues. The nonpolar group was constituted by phenilalanine (PHE), isoleucine (ILE), leucine (LEU), methionine (MET), and valine (VAL). The polar group was constituted by threonine (THR), glutamine (GLN), asparagine (ASN), serine (SER), and cysteine (CYS). The α-helices were acetylated and amidated at their N and C-terminal, respectively, thus rendering them electrically neutral.

Figure 1 shows the structure of polyserine and two types of hydrogen bonds. One type of bond, termed the central hydrogen bonds, was a constitutive part of the α-helix. The other type of hydrogen bonds was termed the lateral hydrogen bonds, a bond that can form between lateral chains or between lateral chains and the backbone of the α-helix. A difference between the polar and the nonpolar groups was that the former gave rise to central hydrogen bonds and lateral hydrogen bonds while the latter only gave rise to central hydrogen bonds.

All simulations were performed with the NAMD Molecular Dynamics Software v.2.9[46] using the CHARMM22[47] potential energy function with CMAP correction. CMAP is an energy correction based on quantum calculations that improves protein backbone behavior and thus yields more accurate prediction of protein structure and dynamics.[48]

The structures were minimized over 10^5 steps and further equilibrated *in vacuo* for 1 ns at a constant temperature of 300 K using Langevin dynamics with a damping coefficient of $\gamma = 5\ ps^{-1}$. An integration time-step of 1 fs was used with a uniform dielectric constant of 1 and a cutoff of nonbonded forces with a switching function that started at a distance of 10 Å and reached zero at 13.5 Å. All of the selected structures kept an α-helical structure without the need for any specific constraints. After this, all the structures were cooled and re-equilibrated to 10 K for 1 ns. Then the heating procedure was applied with this initial temperature of 10 K. Heat was then injected by increasing the kinetic energy of the carbonyl group (C═O) (see Figure 1) at the N-acetyl moiety to a target temperature of 300 K. For this, the same C═O group was subjected to a confining potential of 5 kcal/mol·A^2, and two specific atoms were fixed. These fixed atoms were located in the N-acetylated moiety (carbon atom of the methyl group) and in the C-amidated moiety (nitrogen atom of the amide group). These two atoms, in combination with the

dx.doi.org/10.1021/jp503420e | J. Phys. Chem. B 2014, 118, 10025−10034

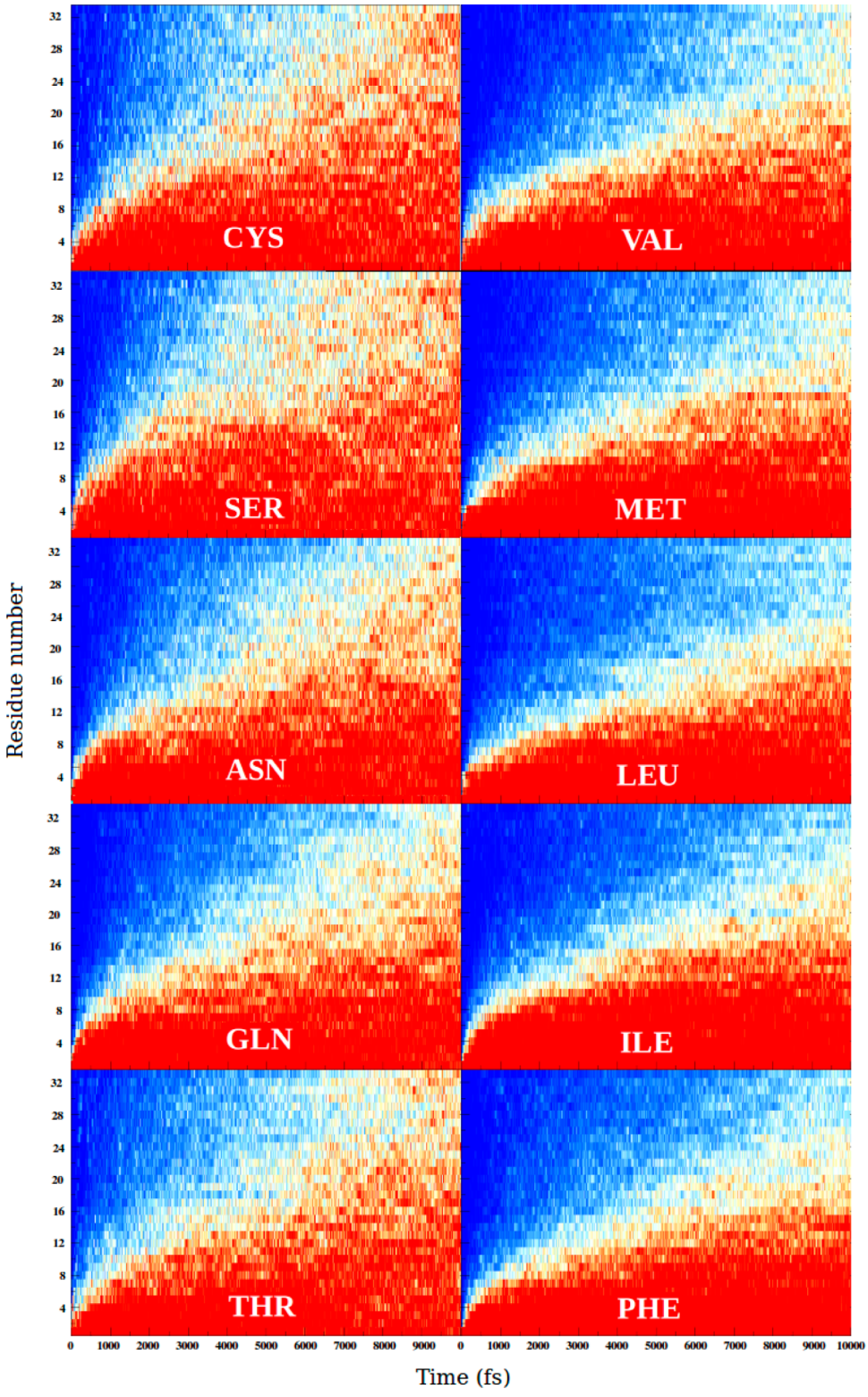

Figure 2. Time dependence of heat diffusion for all analyzed structures. Left column is the polar group. Right column is the nonpolar group. Color scale: red = 300 K, white = 145 K, blue = 10 K.

confining potential of the C═O group, prevented the loss of the helical structure during the heating process. These conditions also avoided the dissipation of energy by internal rotation along the axis connecting the fixed atoms in the N- and C-terminals. The heat flow was determined in selected atoms through a running average of 1000 time-steps. With this data, the average power was computed when needed. Structurally, the formation of total hydrogen bonds, central hydrogen bonds, and lateral hydrogen bonds was measured alongside simulations for both groups. All the simulations were done *in vacuo*. There is experimental evidence that 70% of the injected energy in peptide helices is dissipated to the solvent.[8] Thus, as our interest in this

dx.doi.org/10.1021/jp503420e | *J. Phys. Chem. B* 2014, 118, 10025−10034

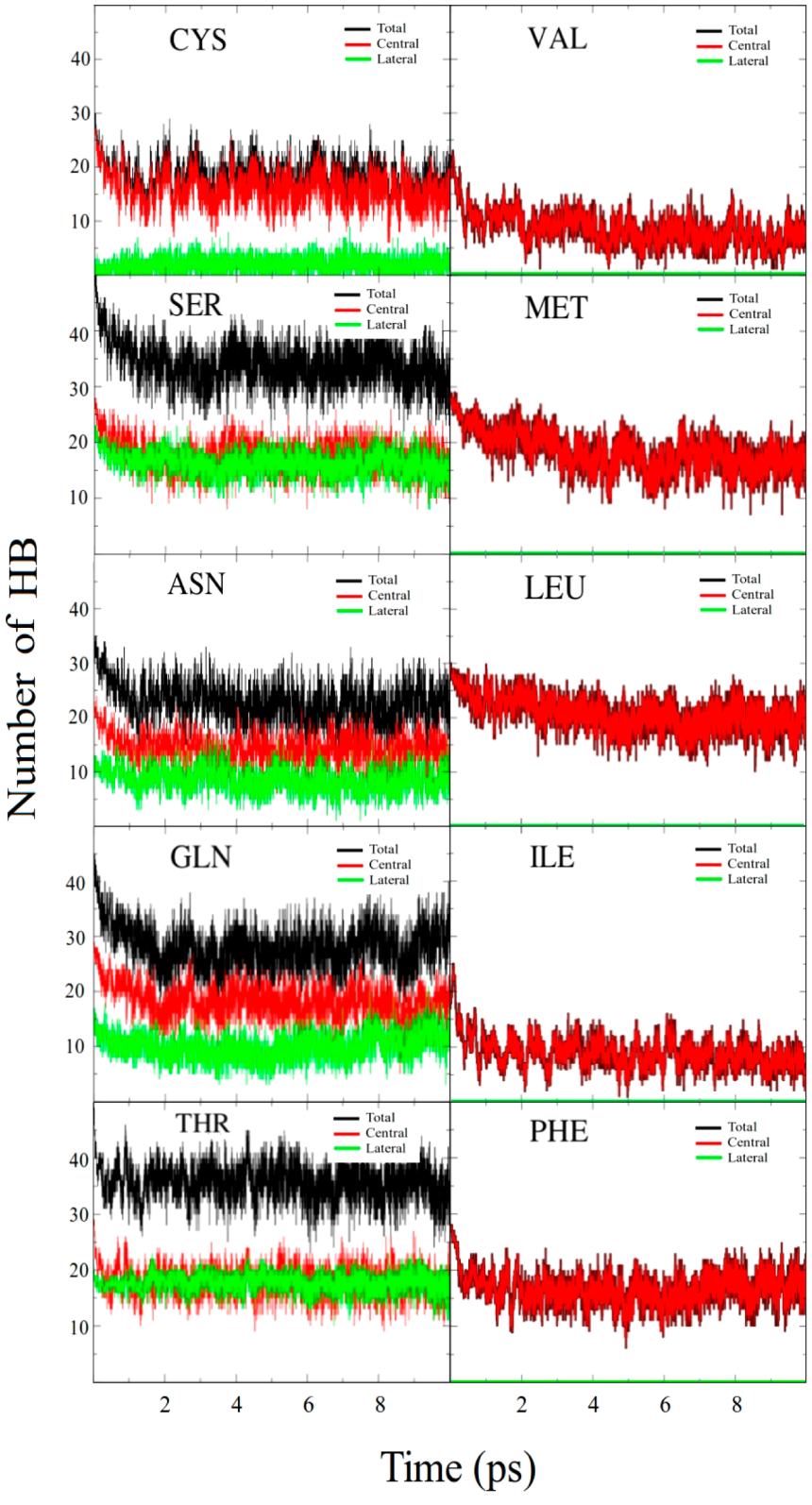

Figure 3. Hydrogen bonds formed during the heating procedure for all structures. Left column is the polar group. Right column is the nonpolar group. Total hydrogen bonds are represented by the black line. Central hydrogen bonds are represented by the red line. Lateral hydrogen bonds are represented by the green line.

work is to study the heat flow through the structure, we chose to do the simulations *in vacuo* to maximize this process. Our model setup seeks to emulate a nonfluxtional α-helix and its response to a local energy excitation.

For use as a comparison, a cooling procedure was also performed. Using the equilibrated structures at 300 K, the kinetic energy was removed. At the same time, the atoms of residues 1 and 33 were coupled to a thermal bath at 0 K. The cooling procedure ran toward a target temperature of 0 K. No constraints

dx.doi.org/10.1021/jp503420e | *J. Phys. Chem. B* 2014, 118, 10025−10034

in position or confining potentials were applied to this set of simulations.

The heating and cooling procedures used the T-couple algorithm of NAMD2. Visualization and data analysis were carried out using the VMD 1.9.1 software.[49]

RESULTS AND DISCUSSION

The time dependence of heat diffusion for the heating procedure of polar and nonpolar groups is shown in Figure 2. These plots give a qualitative picture of the thermal diffusivity along each structure. Moreover, inspection of Figure 2 clearly shows differences between the two groups. In the polar group (left column panel), the high temperature regime (around 300 K) reached the C-terminal site of the protein at 10 000 fs of the simulation time; in the nonpolar group (right column panel), this same temperature regime only reached half of the α-helix. From the beginning of the heating procedure, the polar group showed enhanced diffusivity along the α-helix, and this feature was more pronounced between 5000 and 10 000 fs. Given this, the polar group took less time to transfer heat and thermalize the other side of their respective α-helices.

As the main difference between the analyzed groups was the ability to form hydrogen bonds, these structures were analyzed and quantified during the simulations. Effectively, significant differences were shown through the quantification of hydrogen bonds. Figure 3 shows the number of central hydrogen bonds, lateral hydrogen bonds, and total hydrogen bonds formed by both groups. As can be observed, the polar group (left column panel) formed both central hydrogen bonds and lateral hydrogen bonds, while the nonpolar group (right column) only formed central hydrogen bonds. In general, this gave rise to an increased number of total hydrogen bonds for the polar group. Analysis suggested that the extra hydrogen bonds formed by the polar group was the cause for the observed increase in diffusivity.

In order to gain numerical insight into the heat diffusion process, the average power was determined for the backbone atoms N, O, C, and C_α at residue 28 of each structure in the interval between 0 to 10 000 fs. These results are shown in Table 1. From this determination, the groups were classified into two ranges of average power. The power of the polar group ranked from 364.2 to 285.7 pW, while the power of the nonpolar group ranked from 259.6 to 215.3 pW. No apparent correlation could be made with the molecular weight (MW) of the monomer that composed each α-helix for both groups, but an inverse relation was established between power and the size of the lateral chain. For the nonpolar group, this relation was readily observed, where an increased size of the lateral chain led to a lower average power at position 28. This observation is reminiscent of the dead-end concept, in which a longer or more branched lateral chain leads to a lower power. When taking into account the sequences VAL, LEU, ILE, and PHE, it was possible to follow the bifurcation in atomic connectivity. In the case of MET, an intermediary effect between VAL and LEU was observed.

This effect was also observed in the polar group, in which a more bifurcated side chain was translated in lower power at site 28. Considering the sequence CYS, SER, ASN, and GLN, it was possible to follow the effect of the length of the lateral chain in the measured power at site 28. As the lateral chain increased in length, power decreased. In the case of THR, the bifurcation of a methyl group ($-CH_3$) led to a dead-end that could impose an extra delay in heat transfer to site 28, with a value of 285.7 pW. The replacement of the hydroxyl group ($-OH$) in THR by $-CH_3$ led to VAL of the nonpolar group with a value of 259.6 pW, and this was the next lateral chain after THR in the sequence power measurements at position 28.

Table 1. Name, Structure, Monomer Molecular Weight (MW), and Average Power in the Interval 0 to 10 000 fs for the Backbone Atoms O, N, C, and C_α at Residue 28 for Each Structure

Polar structures			Apolar structures		
Name and structure	Monomer MW (g/mol)	Average power (pW)	Name and structure	Monomer MW(g/mol)	Average power (pW)
CYS 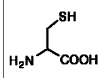	103.15	364.2	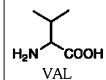 VAL	99.14	259.6
SER 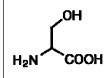	87.09	348.1	MET 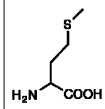	131.19	251.2
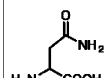 ASN	114.11	335.9	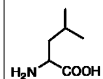 LEU	113.16	239.5
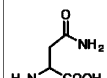 GLN	128.14	306.1	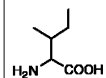 ILE	113.16	237.2
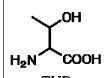 THR	101.11	285.7	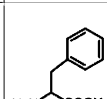 PHE	147.18	215.3

Another comparison was established among members of the two groups that shared a similar MW and degree of ramification. The pairs ASN/LEU and ASN/ILE, which shared a similar MW and ramification, showed increased power for the polar member. The same comparison was applied to the pairs THR/VAL and GLN/MET. These two polar/nonpolar pairs shared a similar MW and bifurcation with the respective polar member, showing a higher average power at the reference position number 28. These comparisons suggest that lateral hydrogen bonds is an important factor in the process of thermalization for these α-helices.

Measuring the kinetic energy of the C_β atom is also useful for characterizing thermalization. The C_β atom connected the backbone of the α-helix to the respective lateral chain (see Figure 1) and appeared in all of the analyzed structures. To provide robust data, measurements at the C_β atom were taken at four consecutive positions in each α-helix, namely, at positions 25, 26, 27, and 28 for each structure. This analysis showed significant differences in both groups (Figure 4). The polar group (left column pannel) showed increased measurements of kinetic energy at this atom, reaching ranges between 1750 and 2000 kcal/mol at 10 000 fs. On the other hand, the nonpolar group (right column pannel) reached energies between 1250 and 1750 kcal/mol at 10 000 fs.

It is very probable that, depending on whether the group is polar or nonpolar, C_β can receive heat from two distinct sources. So, for the nonpolar group C_β atoms received heat flowing along

dx.doi.org/10.1021/jp503420e | J. Phys. Chem. B 2014, 118, 10025−10034

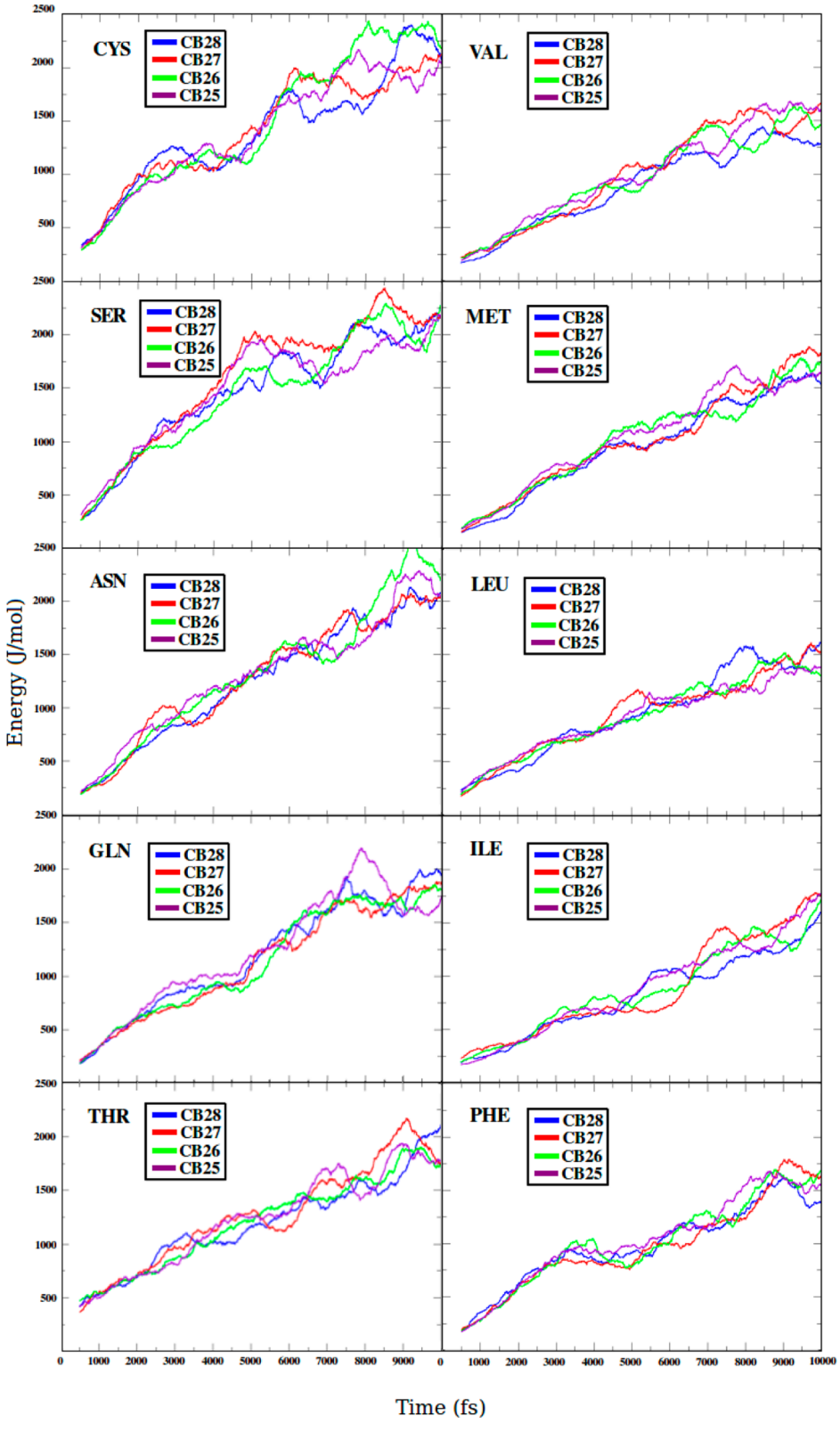

Figure 4. Plots of kinetic energy versus time measured at C_β for residues 25, 26, 27, and 28 for all structures. Left column is the polar group. Right column is the nonpolar group.

the covalent bonds of the backbone of the α-helix and from the associated central hydrogen bonds, while the C_β atoms of the polar group received heat from these sources and also from heat transferred by the lateral hydrogen bonds, thus increasing the rate of heating (Figure 4). In the case of the nonpolar group, the heat reached dead-ends at lateral chains. In contrast, in the polar group lateral hydrogen bonds facilitated the flow of heat to the main axis of the structure or to contiguous lateral chains. By both comparing the data shown in Figures 2, 3, and 4 and in Table 1 and from a general comparison of the structural features of both

dx.doi.org/10.1021/jp503420e | J. Phys. Chem. B 2014, 118, 10025−10034

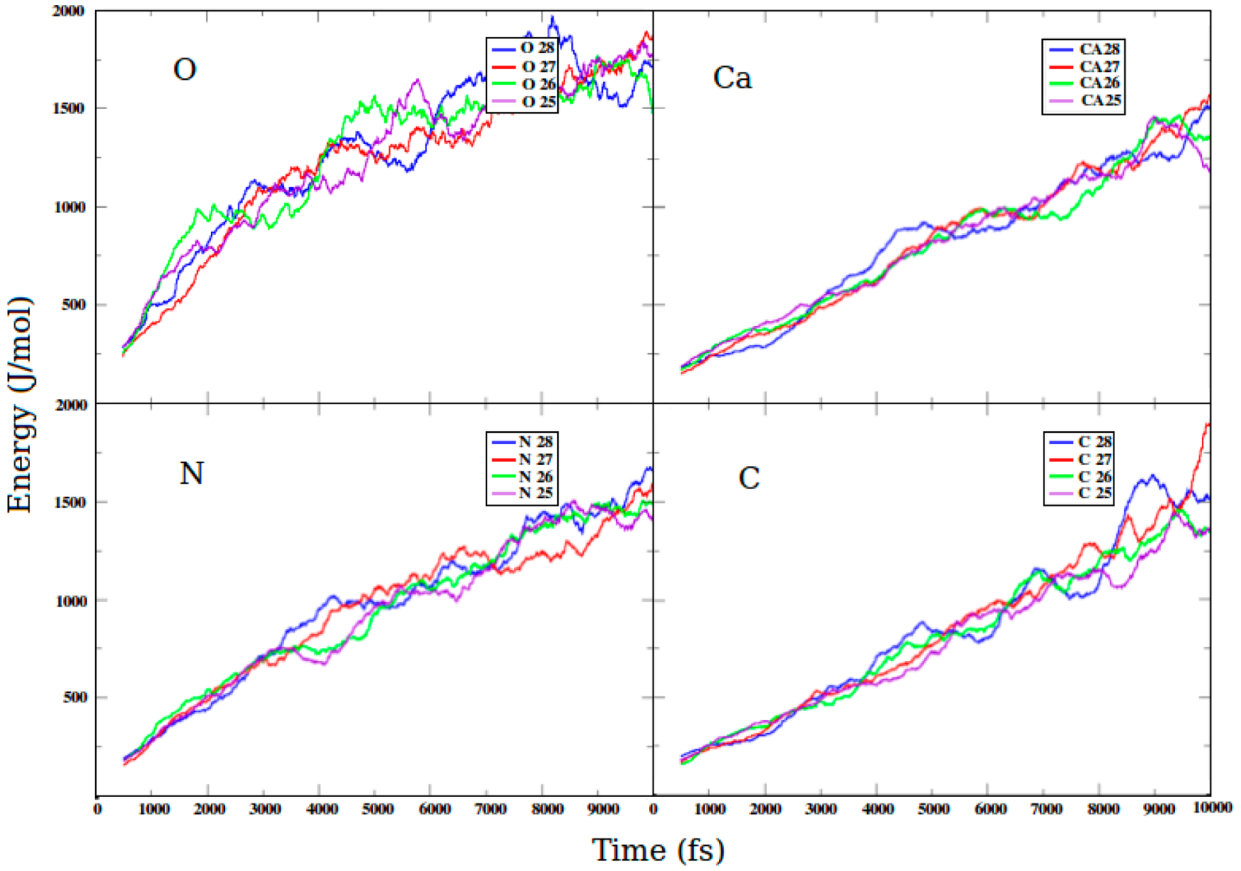

Figure 5. Plots of kinetic energy versus time measured in the atoms O, N, C, and C_α at the backbone positions 25, 26, 27, and 28 of the LEU α-helix.

groups, it is possible to envision the existence of two pathways for heat diffusion. The first pathway could occur through the covalent bonds of the α-helices and through the central hydrogen bonds that are necessary for the occurrence of the α-helical structure. This pathway was common to both groups. The second pathway could occur through lateral hydrogen bonds that were only formed by the polar group. It seems that these lateral hydrogen bonds gave rise to the enhanced heat diffusivity observed in this group. All analyses approximately preserved the trend shown in Table 1, and our results suggest an important role of hydrogen bonds in heat transfer for these α-helical structures and proteins.

Other features of heat conduction along the α-helices were also discovered during research, such as the observation of an energy flow difference in the atoms composing the backbone of O, N, C, and C_α. Using LEU as an example, a plot of kinetic energy versus time at positions 25 to 28 showed that the thermal conductivity followed the order O > N > C ~ C_α (Figure 5). Interestingly, N and O were involved in the formation of central hydrogen bonds in α-helical structures. For comparison, the thermal conductivity for O, N, C, and C_α at position 28 for each member of the polar and nonpolar groups is shown in Figure 6, with results reaffirming the observation that the best thermal conductors along the backbone were O and N, whereas C and C_α showed a lower capability for transferring heat along these structures.

In order to obtain a complete analysis, a cooling procedure was performed, and the results are shown in Figure 7. The results of the cooling procedure showed a trend consistent with the results of the heating procedure (see Table 1), where the nonpolar group presented lower heat diffusivity and the polar group showed higher heat diffusivity. All members of the nonpolar group had higher average temperatures at 10 000 fs as compared to every member of the polar group. Moreover, the relative ordering inside each group was conserved.

CONCLUSIONS

Energy flow in proteins has been correlated with allosteric communication pathways.[6,9] Motivated by this observation, we decided to study heat diffusivity in α-helices by preparing a set of structures with differential abilities to form hydrogen bonds. One group, termed polar, had the ability to form lateral hydrogen bonds, while the group termed nonpolar only formed central hydrogen bonds. The results showed an increased rate of heat diffusivity for α-helices that had the potential to form lateral hydrogen bonds during the heating process, which led to a faster thermalization of the polar group.

It appears that heat reached dead-ends in the lateral chains of the nonpolar group, but the polar group was able to transfer the heat that runs along its lateral chains through lateral hydrogen bonds. In general, the polar group formed more total hydrogen bonds as heating occurred. The number of total hydrogen bonds measured for both groups showed a qualitative correlation with the average heat rate measured at position 28 for all α-helices (Table 1). This correlation can also be observed by comparing the data presented in Figures 2 and 3.

A good indicator of the differences in thermal flow between both groups is the heating of C_β, which was located between C_α and the lateral chains in all analyzed helices. The heat rate of C_β was measured at four different positions −25, 26, 27, and 28. The results demonstrated that the rate of heating was always higher

dx.doi.org/10.1021/jp503420e | J. Phys. Chem. B 2014, 118, 10025−10034

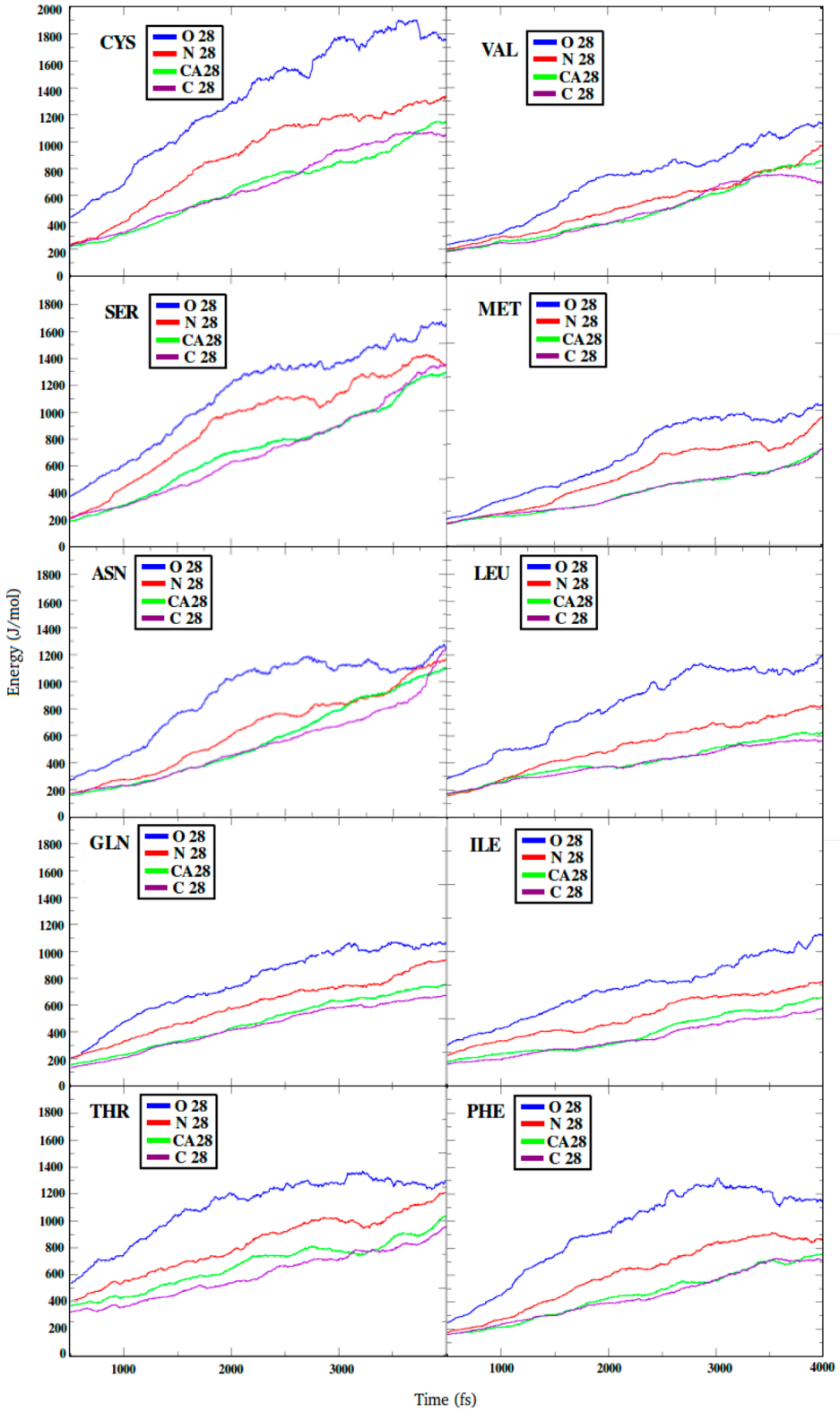

Figure 6. Plots of kinetic energy versus time measured in the atoms O, N, C, and C_α at the backbone position 28 of all α-helices. Left column is the polar group. Right column is the nonpolar group.

for the polar group (Figure 4). Due to the structural differences between both groups, it was quite probable that the C_β from the polar group received heat from two pathways. The first pathway followed the backbone of the α-helix and its respective hydrogen bonds, and the second pathway arose from the lateral hydrogen bonds that can only be formed by this group. In the case of the nonpolar group, C_β was only heated by the first pathway. This would explain the results observed in Figure 4, and it is moreover consistent with the results shown in Figures 2 and 3 and in Table 1.

Moreover, different atoms showed a differential capability to transfer heat, with O and N acting as better conductors than C

dx.doi.org/10.1021/jp503420e | J. Phys. Chem. B 2014, 118, 10025−10034

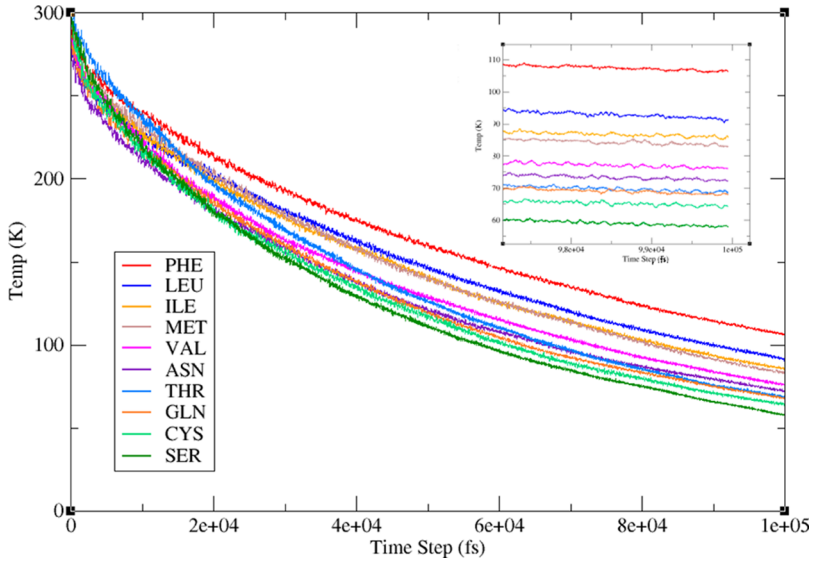

Figure 7. Average temperature determined at each time-step for the cooling procedure in each structure. The inset shows the detail of the end of the cooling procedure. The nonpolar group demonstrated lower heat diffusivity, which was reflected by a higher average temperature at 10 000 fs.

and C_α. This effect was detected in all analyzed structures. Interestingly, O and N are involved in the formation of hydrogen bonds, thus suggesting that hydrogen bonds are better heat conductors than covalently linked atoms such as C and C_α. In order to provide complete data, a cooling procedure was performed. This procedure showed a coherent, similar trend to the heating procedure, and the polar group lost heat at an increased rate compared to the nonpolar group.

Our results show some overlap with the Davydov model.[3] This model gives a role to the amide I vibration in the propagation of energy in peptide helices. The amide I vibration involves vibration of the peptide bond CONH atoms that form a structural part of the hydrogen bonds in the backbone structure of the helices. While at low temperatures both the classical and the semiclassical regimes differ from the full quantum Davydov system,[4] the coincidence of our molecular dynamic simulations with the predictions of the full quantum Davydov system makes us think that a purely classical model may suffice. However, this report does not seek to refute or support the soliton model of Davidov, but studies the role that hydrogen bonds could have in the propagation of vibrational energy in α-helices. Our results are in direct concordance with recent reports about the role of hydrogen bonds in the heat diffusion in structural patterns of proteins, such as β-sheets.[33]

We conclude that the increased rate of heating observed in this study is a function of the number of hydrogen bonds formed as heat transfer takes place. This would differentiate the two groups, and heat would flow faster through atoms involved in hydrogen bonds. Also, an analysis of the structural differences in all members of both groups showed that the length and bifurcation of the lateral chains was an important factor in the observed heat rates.

As a general conclusion, we suggest that hydrogen bonds play an important role in thermal transfer in proteins, which implies their importance in signal propagation in proteins. Future studies by our group will focus on models of allosteric proteins so as to make exact correlations between allosteric pathways and the structural determinants associated with these communication pathways.

AUTHOR INFORMATION

Corresponding Author

*Mailing address: República 239, 3er piso, Santiago, Chile. Phone: +562 2770 3612. E-mail: germino@u.uchile.cl; german.mino.galaz@gmail.com. Website: www.gnm.cl.

Notes

The authors declare no competing financial interest.

ACKNOWLEDGMENTS

The authors would like to acknowledge funding by FONDECYT Grant 3110149 (awarded to G.M.) and partial support of FONDECYT Regular 1120603 (awarded to G.G.). This work was also supported by grants from the Millennium Initiative (P09-022-F), Conicyt Proyecto Anillo ACT - 1104.

REFERENCES

(1) Leitner, D. M.; Straub, J. E., Eds. *Proteins: Energy, Heat and Signal Flow*; Taylor and Francis Group: New York, 2010.

(2) Piazza, F.; Sanejouand, Y. H. Discrete breathers in protein structures. *Phys. Biol.* **2008**, *5*, 026001.

(3) Davydov, A. S. Solitons and energy transfer along protein molecules. *J. Theor. Biol.* **1977**, *66*, 379−387.

(4) Cruzeiro-Hansson, L.; Takeno, S. Davydov model: The quantum, mixed quantum-classical, and full classical Systems. *Phys. Rev. E* **1997**, *56*, 894.

(5) Mimshe Fewu, J. C.; Tabi, C. B.; Edongue, H.; Ekobena Fouda, H. P.; Kofané, T. C. Wave patterns in α-helix proteins with interspine coupling. *Phys. Scr.* **2013**, *87*, 025801.

(6) Leitner, D. M. Energy flow in proteins. *Annu. Rev. Phys. Chem.* **2008**, *59*, 233−259.

(7) Leitner, D. M. Frequency-resolved communication maps for proteins and other nanoscale materials. *J. Chem. Phys.* **2009**, *130*, 195101.

(8) Gnanasekaran, R.; Agbo, J. K.; Leitner, D. M. Communication maps computed for homodimeric hemoglobin: Computational study of water-mediated energy transport in proteins. *J. Chem. Phys.* **2011**, *135*, 065103.

(9) Ota, N.; Agard, D. A. Intramolecular signaling pathways revealed by modeling anisotropic thermal diffusion. *J. Mol. Biol.* **2005**, *351*, 345−354.

(10) Liu, J.; Tawa, G. J.; Wallqvist, A. Identifying cytochrome p450 functional networks and their allosteric regulatory elements. *PLoS One* **2013**, *8*, e81980.
(11) Burendahl, S.; Nilsson, L. Computational studies of LXR molecular interactions reveal an allosteric communication pathway. *Proteins* **2012**, *80*, 294−306.
(12) Laine, E.; Auclair, C.; Tchertanov, L. Allosteric communication across the native and mutated KIT receptor tyrosine kinase. *PLoS Comput. Biol.* **2012**, *8*, e1002661.
(13) Noinaj, N.; Bhasin, S. K.; Song, E. S.; Scoggin, K. E.; Juliano, M. A.; Juliano, L.; Hersh, L. B.; Rodgers, D. W. Identification of the allosteric regulatory site of insulysin. *PLoS One* **2011**, *6*, e20864.
(14) Seldeen, K. L.; Deegan, B. J.; Bhat, V.; Mikles, D. C.; McDonald, C. B.; Farooq, A. Energetic coupling along an allosteric communication channel drives the binding of Jun-Fos heterodimeric transcription factor to DNA. *FEBS J.* **2011**, *278*, 2090−104.
(15) Ackers, G. K.; Hazzard, J. H. Transduction of binding energy into hemoglobin cooperativity. *Trends Biochem. Sci.* **1993**, *18*, 385−90.
(16) Koshland, D. E., Jr.; Némethy, G.; Filmer, D. Comparison of experimental binding data and theoretical models in proteins containing subunits. *Biochemistry* **1966**, *5*, 365−85.
(17) Monod, J.; Wyman, J.; Changeux, J. P. On the nature of allosteric transitions: A plausible model. *J. Mol. Biol.* **1965**, *12*, 88−118.
(18) Fuentes, E. J.; Gilmore, S. A.; Mauldin, R. V.; Lee, A. L. Evaluation of energetic and dynamic coupling networks in a PDZ domain protein. *J. Mol. Biol.* **2006**, *364*, 337−51.
(19) Jiao, W.; Parker, E. J. Using a combination of computational and experimental techniques to understand the molecular basis for protein allostery. *Adv. Protein. Chem. Struct. Biol.* **2012**, *87*, 391−413.
(20) Gianni, S.; Walma, T.; Arcovito, A.; Calosci, N.; Bellelli, A.; Engström, A.; Travaglini-Allocatelli, C.; Brunori, M.; Jemth, P.; Vuister, G. W. Demonstration of long-range interactions in a PDZ domain by NMR, kinetics, and protein engineering. *Structure.* **2006**, *14*, 1801−1809.
(21) Popovych, N.; Sun, S.; Ebright, R. H.; Kalodimos, C. G. Dynamically driven protein allostery. *Nat. Struct. Mol. Biol.* **2006**, *13*, 831−838.
(22) Lockless, S. W.; Ranganathan, R. Evolutionarily conserved pathways of energetic connectivity in protein families. *Science* **1999**, *286*, 295−299.
(23) Rivalta, I.; Sultan, M. M.; Lee, N. S.; Manley, G. A.; Loria, J. P.; Batista, V. S. Allosteric pathways in imidazole glycerol phosphate synthase. *Proc. Natl. Acad. Sci. U. S. A.* **2012**, *109*, E1428−36.
(24) Sharp, K.; Skinner, J. J. Pump-probe molecular dynamics as a tool for studying protein motion and long range coupling. *Proteins* **2006**, *65*, 347−361.
(25) Kong, Y.; Karplus, M. Signaling pathways of PDZ2 domain: A molecular dynamics interaction correlation analysis. *Proteins* **2009**, *74*, 145−154.
(26) Li, G.; Magana, D.; Dyer, R. B. Anisotropic energy flow and allosteric ligand binding in albumin. *Nat. Commun.* **2014**, *5*, 3100.
(27) Buchli, B1; Waldauer, S. A.; Walser, R.; Donten, M. L.; Pfister, R.; Blöchliger, N.; Steiner, S.; Caflisch, A.; Zerbe, O.; Hamm, P. Kinetic response of a photoperturbed allosteric protein. *Proc. Natl. Acad. Sci. U. S. A.* **2013**, *110*, 11725−11730.
(28) Lervik, A.; Bresme, F.; Kjelstrup, S.; Bedeaux, D.; Miguel Rubi, J. Heat transfer in protein-water interfaces. *Phys. Chem. Chem. Phys.* **2010**, *12* (7), 1610−7.
(29) Kjelstrup, S.; Rubi, J. M.; Bedeaux, D. Energy dissipation in slipping biological pumps. *Phys. Chem. Chem. Phys.* **2005**, *7*, 4009−4018.
(30) Helbing, J.; Devereux, M.; Nienhaus, K.; Nienhaus, G. U.; Hamm, P.; Meuwly, M. Temperature dependence of the heat diffusivity of proteins. *J. Phys. Chem. A* **2012**, *116*, 2620−8.
(31) Botan, V.; Backus, E. H.; Pfister, R.; Moretto, A.; Crisma, M.; Toniolo, C.; Nguyen, P. H.; Stock, G.; Hamm, P. Energy transport in peptide helices. *Proc. Natl. Acad. Sci. U. S. A.* **2007**, *104*, 12749−12754.
(32) Sagnella, D. E.; Straub, J. E. Directed Energy "Funneling" Mechanism for Heme Cooling Following Ligand Photolysis or Direct Excitation in Solvated Carbonmonoxy Myoglobin. *J. Phys. Chem. B* **2001**, *105*, 7057−7063.
(33) Zhang, L.; Chen, T.; Bana, H.; Liu, L. Hydrogen bonding-assisted thermal conduction in β-sheet crystals of spider silk protein. *Nanoscale* **2014**, *6*, 7786−7791.
(34) Schoena, P. A. E.; Michelb, B.; Curionib, A.; Poulikakosa, D. Hydrogen-bond enhanced thermal energy transport at functionalized, hydrophobic and hydrophilic silica−water interfaces. *Chem. Phys. Lett.* **2009**, *476*, 271−276.
(35) Lin, Z.; Rubtsov, I. V. Constant-speed vibrational signaling along polyethyleneglycol chain up to 60-Å distance. *Proc. Natl. Acad. Sci. U. S. A.* **2012**, *109*, 1413−1418.
(36) Kjelstrup, S.; Rubi, J. M.; Bedeaux, D. Energy dissipation in slipping biological pumps. *Phys. Chem. Chem. Phys.* **2005**, *7*, 4009−4018.
(37) Pimentel, G. C.; McClellan, L. *The Hydrogen Bond*; W. H. Freeman and Company: San Francisco and London, 1960.
(38) Nick Pace, C.; Scholtz, J. M.; Grimsley, G. R. Forces stabilizing proteins. *FEBS Lett.* **2014**, *588*, 2177−2184.
(39) Lomdahl, P. S.; Kerr, W. C. Do Davydov Solitons Exist at 300 K? *Phys. Rev. Lett.* **1985**, *55*, 1235.
(40) Martínez, L.; Figueira, A.; Webb, P.; Polikarpov, I.; Skaf, M. S. Mapping the Intramolecular Vibrational Energy Flow in Proteins Reveals Functionally Important Residues. *J. Phys. Chem. Lett.* **2011**, *2*, 2073−2078.
(41) Weinhold, F.; Landis, C. *Valency and Bonding: A Natural Bond Orbital Donor−Acceptor Perspective*; Cambridge University Press: Cambridge, 2005.
(42) Lopes Jesus, A. J.; Redinha, J. S. Charge-assisted intramolecular hydrogen bonds in disubstituted cyclohexane derivatives. *J. Phys. Chem. A* **2011**, *115*, 14069−14077.
(43) Frey, P. A.; Whitt, S. A.; Tobin, J. B. A low-barrier hydrogen bond in the catalytic triad of serine proteases. *Science* **1994**, *264*, 1927−30.
(44) Miño, G.; Contreras, R. On the role of short and strong hydrogen bonds on the mechanism of action of a model chymotrypsine active site. *J. Phys. Chem. A* **2009**, *113*, 5769−5772.
(45) Mino, G.; Contreras, R. Non-electrostatic components of short and strong hydrogen bonds induced by compression inside fullerenes. *Chem. Phys. Lett.* **2010**, *486*, 119−122.
(46) Kale, L.; Skeel, R.; Bhandarkar, M.; Brunner, R.; Gursoy, A.; Krawetz, N.; Phillips, J.; Shinozaki, A.; Varadarajan, K.; Schulten, K. NAMD2: Greater scalability for parallel molecular dynamics. *J. Comput. Phys.* **1999**, *151*, 283−312.
(47) MacKerell, A. D., Jr; Bashford, D.; Bellott, M.; Dunbrack, R. L., Jr.; Evanseck, J.; Field, M. J.; Fischer, S.; Gao, J.; Guo, H.; Ha, S.; et al. All-atom empirical potential for molecular modeling and dynamics studies of proteins. *J. Phys. Chem. B* **1998**, *102*, 3586−3616.
(48) Mackerell, A. D., Jr.; Feig, M.; Brooks, C. L., 3rd. Extending the treatment of backbone energetics in protein force fields: limitations of gas-phase quantum mechanics in reproducing protein conformational distributions in molecular dynamics simulations. *J. Comput. Chem.* **2004**, *25*, 1400−1415.
(49) Humphrey, W.; Dalke, A.; Schulten, K. VMD—Visual molecular dynamics. *J. Mol. Graph.* **1996**, *14*, 33−38.